Available online at www.sciencedirect.com

SciVerse ScienceDirect

Ceramics International 38 (2012) 6445–6453

CERAMICS INTERNATIONAL

www.elsevier.com/locate/ceramint

Synthesis and reaction mechanism of Ti_3SiC_2 ternary compound by carbothermal reduction of TiO_2 and SiO_2 powder mixtures

Senol Cetinkaya*, Serafettin Eroglu

Istanbul University, Engineering Faculty, Department of Metallurgical and Materials Eng., Avcilar 34320, Istanbul, Turkey

Received 2 April 2012; received in revised form 7 May 2012; accepted 8 May 2012
Available online 19 May 2012

Abstract

The present study aims to investigate synthesis of Ti_3SiC_2 from TiO_2 and SiO_2 powder mixtures by carbothermal reduction method. Equilibrium TiO_2–SiO_2–C ternary phase diagram was used to predict the conditions for the formation of Ti_3SiC_2 at 1800 K under Ar atmosphere. A reactant mixture with a TiO_2:SiO_2 molar ratio of 1.5 and a C content of 68.75 mol% (26.86 wt%) was initially selected among the thermodynamically favorable reactant compositions for the experimental studies. Two different C sources, graphite flakes and pyrolytic C coating, were used to synthesize Ti_3SiC_2 at 1800 K under Ar atmosphere. When graphite flakes were used, the products contained a trace amount of Ti_3SiC_2 phase along with major TiC and minor SiC phases. Whereas, pyrolytic C coating on the oxide particles resulted in the products with much higher Ti_3SiC_2 contents owing to the close contact between the reactants. Optimal C concentration for the C coated oxide mixtures with a TiO_2:SiO_2 molar ratio of 1.5 was determined to be 30.05 wt% under the experimental conditions studied. Ti_3SiC_2 content of the products obtained from this reactant was observed to increase with reaction time to 31 wt% at 75 min beyond which it gradually decreased. XRD studies indicated that the product with the highest ternary carbide content also contained TiC and a trace amount of SiC. SEM-EDS analyses showed that this sample essentially consisted of spherical fine TiC particles and Ti_3SiC_2 nanolaminates. Equilibrium thermodynamic analysis of the TiO_2–SiO_2–C system suggested that the reaction of solid Ti_2O_3 with SiO and CO gases may play a dominant role in the formation of Ti_3SiC_2.

Keywords: A. Powders: gas phase reaction; Carbothermal reduction; Ti_3SiC_2 ternary carbide

1. Introduction

Ternary titanium silicon carbide (Ti_3SiC_2) compound with a layered hexagonal structure is the most popular member of the $M_{n+1}AX_n$ phases ($n=1$, 2 or 3) where M is an early transition metal, A is a group A element and X is C and/or N. Ti_3SiC_2 has received considerable attention because it offers unusual combination of metallic and ceramic properties. For example, it is readily machinable, thermally shock resistant, electrically conductive and has a low density, a high melting point, good oxidation resistance. Hence, Ti_3SiC_2 has been considered a potential material for high temperature applications such as bearings, engine linings, turbine blades in aircraft and diesel engines [1–4].

Various methods have been developed for the synthesis of Ti_3SiC_2 including arc-melting [5], chemical vapor deposition [6], hot-isostatic pressing [7], spark plasma sintering [8], pulse discharge sintering [9], mechanically activated sintering [10], plasma spraying [11] and self propagating high temperature synthesis [12]. All these methods, however, use combinations of high cost non-oxide precursors (e.g. Ti, Si, TiC, SiC, $TiCl_4$, CH_3SiCl_3). Furthermore, these techniques involve complex, time consuming processes or corrosive reactants.

No report has been published on the synthesis of Ti_3SiC_2 from oxide precursors (TiO_2 and SiO_2) by carbothermal reduction method. In addition, equilibrium thermodynamic analysis has not been carried out in the TiO_2–SiO_2–C system. Hence, the objectives of the present study were (i) to synthesize Ti_3SiC_2 compound from the oxide

*Corresponding author. Tel.: +90 212 473 7070x17759; fax: +90 212 473 7180.
E-mail address: senol-c@istanbul.edu.tr (S. Cetinkaya).

0272-8842/$36.00
http://dx.doi.org/10.1016/j.ceramint.2012.05.020

reactants and (ii) to predict process parameters and to understand reaction pathways leading to the formation of the ternary carbide by thermodynamic analysis.

2. Thermodynamic analysis

Equilibrium thermodynamic analysis was performed by the method of minimization of the Gibbs' free energy [13] of the Ti–Si–O–C–Ar system using a modified version of Eriksson's computer program SOLGASMIX [14] at atmospheric pressure. In the system of interest, 24 species were considered for the constituents of the gas phase including Ar, TiO_2, TiO, Ti, SiO_2, SiO, Si, SiC_2, Si_2C, O, O_2, CO and CO_2. Condensed equilibrium phases were assumed to be C, TiO_2, titanium sub-oxides (Ti_4O_7, Ti_3O_5, Ti_2O_3 and TiO), Ti, TiC, SiO_2, Si, α-SiC, β-SiC, TiSi, $TiSi_2$, Ti_5Si_3 and Ti_3SiC_2. Input thermodynamic data in the form of Gibbs' free energy of the formation of the constituents were obtained from the published literature [1,15,16].

Thermodynamic calculations were initially carried out for a constant TiO_2:SiO_2 molar ratio of 3 corresponding to the stoichiometric Ti:Si ratio in Ti_3SiC_2. The analysis was done at temperatures between 1500 and 1800 K for input C mole fraction (X_C) ranging from zero to unity for a TiO_2:Ar molar ratio of 0.006. X_C was defined as $n^o_C/(n^o_{TiO_2}+n^o_{SiO_2}+n^o_C)$, where n^o represents molar amounts of the reactants.

Fig. 1 shows a stability diagram for the condensed phases obtained from the thermodynamic analysis. The boundary lines in the diagram divide different phase fields (represented by numbers) in which the indicated phases are expected to form. The information obtained from the figure can be summarized as follows. Oxide phases are progressively reduced and transformed to the carbide phases with increasing X_C. Single Ti_3SiC_2 phase is not expected to form under the conditions studied as seen from the diagram. It is, however, predicted that the ternary carbide phase co-exists with other phases (Ti_2O_3, SiO_2, TiC and SiC) as shown by the phase fields of 9–13 and 17–19 at input C mole fractions roughly in the range 0.30–0.75 and at the temperatures above ~1600 K.

Further thermodynamic analysis was carried out to determine if single Ti_3SiC_2 phase forms in the Ti–Si–O–C–Ar system at 1800 K. Hence, a ternary TiO_2–SiO_2–C phase diagram was constructed for a TiO_2:Ar molar ratio of 0.006. Fig. 2 shows the ternary diagram displaying condensed phases in equilibrium with the gas phase. As can be seen from the figure, single phase Ti_3SiC_2 is only predicted along the line numbered 20 corresponding to the C-rich region with input TiO_2:SiO_2 molar ratios in the range of 0.25–1.90. As the TiO_2:SiO_2 molar ratio varies from 0.25 to 1.90, the C content of the input reactant required for pure Ti_3SiC_2 formation increases from 58.33 to 69.80 mol%, respectively. Among the thermodynamically favorable reactant compositions, a reactant mixture with a molar composition of 18.75% TiO_2–12.50% SiO_2–68.75% C was initially selected for the experimental studies. It should be noted that this composition corresponds to a TiO_2:SiO_2:C molar ratio of 3:2:11.

3. Experimental procedures

The synthesis experiments were carried out in a horizontal tubular furnace equipped with SiC heating elements, an alumina tube (20 mm in diameter, 500 mm in length) and gas flow meters. The chemicals used were SiO_2 (99.5%), TiO_2 (99.7%), graphite powder, high purity Ar (99.999%) and CH_4 (99.5%). Particle sizes of the TiO_2 and SiO_2 powders were reported to be <25 nm and 10–20 nm, respectively, by the producer (Sigma-Aldrich).

Two different C sources, graphite flakes and C coating, were used for the carbothermal reduction of the oxides. Hence, two routes were followed to prepare the initial reactant mixtures prior to carbothermal reduction.

In the first route, graphite was used as a carbon source. TiO_2 (48.71 wt%) and SiO_2 (24.43 wt%) powders and graphite flakes (26.86 wt%) were weighed to give the desired molar ratio of 3:2:11 as predicted by thermodynamic analysis. Mixing of the reactants was carried out in ethanol using a magnetic stirrer. Ethanol was then evaporated in an oven at 373 K.

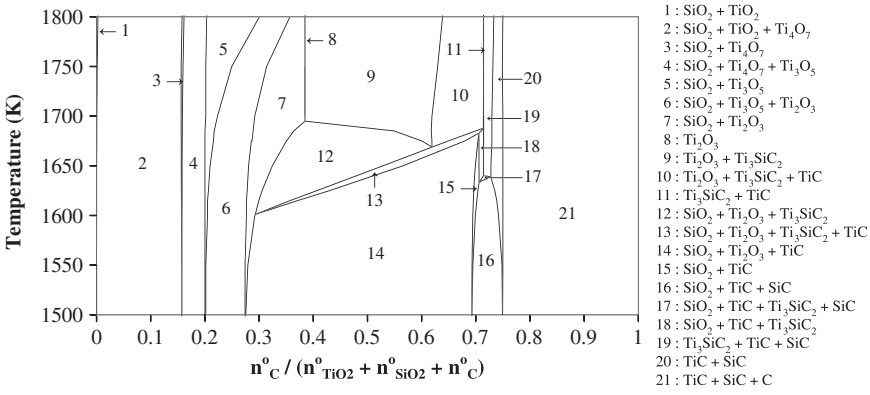

Fig. 1. Equilibrium solid stability diagram showing phase fields as a function of temperature and input carbon mole fraction. Input TiO_2:SiO_2 and TiO_2:Ar molar ratios are kept constant at 3 and 0.006, respectively.

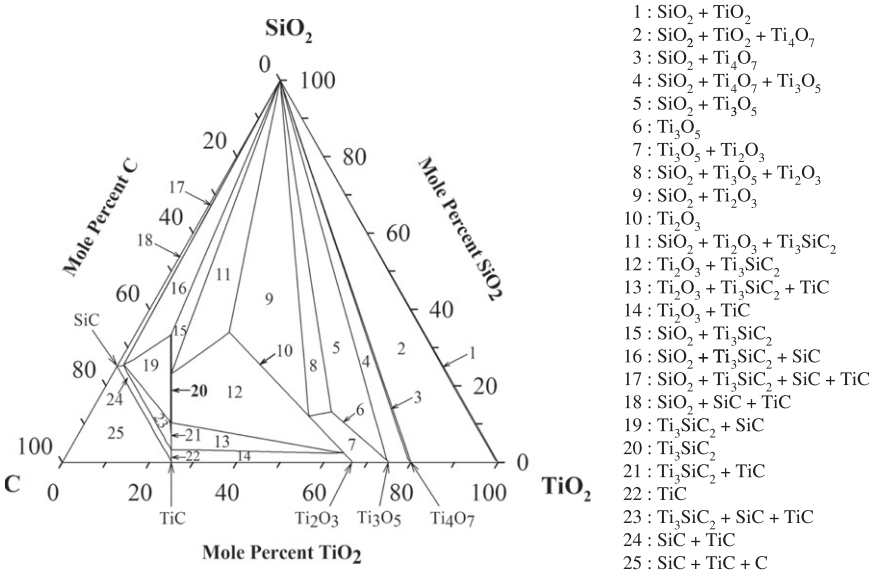

Fig. 2. TiO_2–SiO_2–C ternary phase diagram displaying condensed phases in equilibrium with the gas phase at 1800 K. Input TiO_2:Ar molar ratio is 0.006.

In the second route, pyrolytic carbon coating was grown on the oxide particles by chemical vapor deposition technique. The deposition process was carried out as follows. TiO_2 and SiO_2 powders with a molar ratio of 3:2 were initially mixed in ethanol and the mixture was then dried. The oxide mixture of ~150 mg was placed in the hot zone of the furnace. CH_4 was allowed to flow (40 cm^3/min) through the furnace tube during heating at a rate 25 K/min to 1300 K to minimize sintering of the oxide nanoparticles. When 1300 K was reached, the powders were isothermally held for various periods of time (0–15 min) to deposit various amounts of C. Carbon content of the coated samples was determined from mass changes after burning carbon in air at 900 K for ~15 min. Mass measurements were carried out by a calibrated electronic balance (Sartorius BP110S) with a sensitivity of $\pm 10^{-4}$ g.

For carbothermal reduction experiments, the initial masses of the reactants used were ~150 mg and ~200 mg for the oxide mixture with graphite flakes and carbon coated oxide mixtures, respectively. The samples were heated to 1800 K at a rate of 40 K/min under Ar flow (250 cm^3/min) and held at this temperature for various periods of time. All products were cooled in Ar atmosphere.

Morphology of the C coated particles was examined by a High Resolution Transmission Electron Microscope (JEOL 2100 LaB_6 HR-TEM). A Field Emission Gun Scanning Electron Microscope (FEI Quanta FEG 450) equipped with Energy dispersive X-rays spectrometer (EDS) was used to study morphology and composition of the powders after carbothermal reaction. Mean particle sizes of the products were determined from at least 70 measurements using the FEG-SEM images. A parafocusing X-ray diffractometer (RIGAKU D/Max-2200 XRD) equipped with a Cu radiation tube (λ=0.15418 nm), and a monochrometer was used for phase analysis of the powders.

4. Results and discussion

4.1. Carbothermal reduction of the oxide mixture with graphite flakes

Fig. 3 displays XRD patterns of the starting powder mixture and the products obtained at 1800 K for isothermal holding times ranging from 0 to 90 min. The pattern of the starting powder mixture reveals minor rutile and major anatase phases with broad diffraction peaks. A sharp peak from the (002) crystallographic plane of graphite is also seen at ~26.7°. Absence of SiO_2 peaks from the pattern is attributed to poorly crystalline small particles. The XRD pattern of the sample obtained at 0 min reveals the following information. The product essentially consists of TiC phase containing some oxygen. The peak from the (101) crystallographic plane of cristobalite-tetragonal SiO_2 appears at 22° because of increased crystallinity during heating. In addition, there are diffraction peaks with slight intensities from TiO_2 (rutile), titanium sub-oxide, SiC and C phases. With an increase in holding time, the intensities of the peaks from the oxide and C phases gradually disappear as can be seen from the relevant patterns. In addition, the diffraction angles of TiC peaks shift to lower angles, indicating that oxygen content of the product decreases [17]. At 60 min, weak diffraction peaks from (101), (104) and (105) crystal planes of hexagonal Ti_3SiC_2 phase appears at 34.1°, 39.5° and 42.5°, respectively. When reaction time is increased to 90 min, a slight decrease in the intensities of these peaks can be seen from the respective pattern. These results indicate that carbothermal reduction

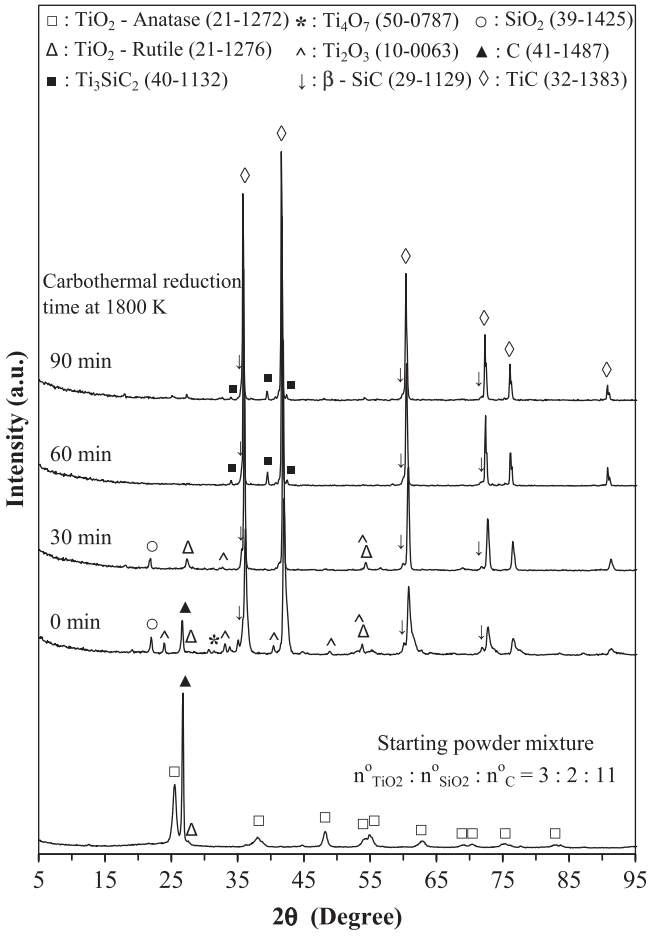

Fig. 3. X-ray diffraction patterns of the starting powder mixture with graphite flakes and the products obtained at 1800 K for carbothermal reduction times in the range 0–90 min.

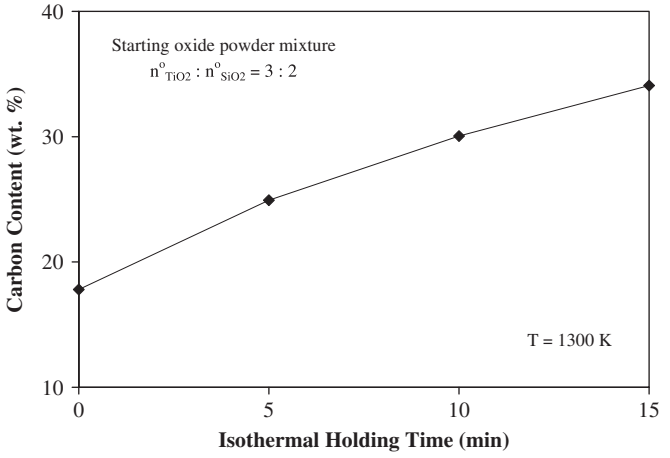

Fig. 4. Effect of isothermal holding time on the carbon contents of the products. The starting oxide mixture was heated to 1300 K and held at this temperature in a flowing CH_4 atmosphere.

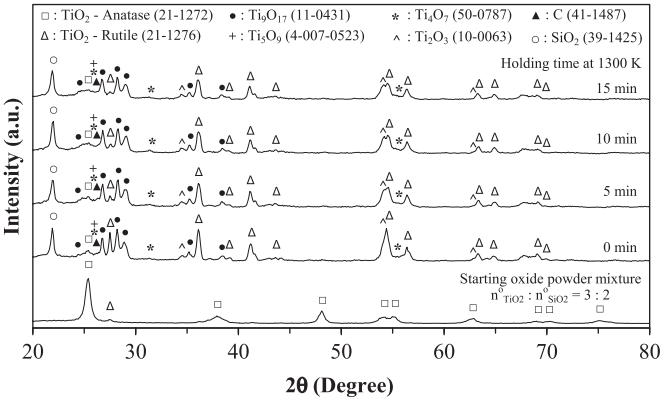

Fig. 5. XRD patterns of the starting oxide mixture and the products obtained after heating to 1300 K and holding at this temperature for 0–15 min in a flowing CH_4 atmosphere.

of the oxide mixture by graphite flakes does not yield a significant amount of Ti_3SiC_2 phase.

4.2. Carbothermal reduction of the oxide particles coated with pyrolytic carbon

4.2.1. Deposition of pyrolytic carbon

A close contact between C and the oxide particles may enhance formation of Ti_3SiC_2 compound. This was achieved by chemical vapor deposition of C from CH_4 on the mixed oxide particles. Fig. 4 shows effect of isothermal holding time on C content of the products at 1300 K. As can be seen from the figure, the amount of C deposited increases from 17.81 wt% at 0 min to 34.08 wt% at 15 min. XRD patterns of the starting oxide mixture and the products are displayed in Fig. 5. The pattern of the starting oxide mixture consists of only TiO_2 (major anatase and minor rutile phases) diffraction peaks. After the deposition process, SiO_2 peak from the crystallographic plane of (101) appears at 22° due to increased crystallinity. Furthermore, anatase mostly transformed to rutile as expected. The presence of titanium sub-oxide (Ti_9O_{17}, Ti_5O_9, Ti_4O_7, Ti_2O_3) peaks and a decrease in the intensity of TiO_2 (rutile) peak at 36.1° with increasing reaction time indicate that TiO_2 was partially reduced by CH_4. It is also noticed from the patterns that $C_{(002)}$ peak at ~26.5° overlaps with those of titanium sub-oxides.

Fig. 6 displays the HR-TEM images at various magnifications for the product obtained from the oxide mixture after heating to 1300 K and holding at this temperature for 10 min in CH_4 atmosphere. The oxide particle size measured from the multiple images (Fig. 6a and b) were found to be in the range of 50–120 nm indicating that sintering of particles took place during the deposition process. As can be seen from the HR-TEM images (Fig. 6c and d), the oxide particles were coated with pyrolytic carbon layers with thicknesses in the range of 5–20 nm. The interplanar spacing in the layers was determined to be 0.340 nm slightly higher than that of the (002) crystallographic plane of single crystal graphite (0.336 nm). This result is attributable to microstrains caused by growth stress and thermal stress originating from the differential thermal contraction between the coating and the oxide during cooling stage.

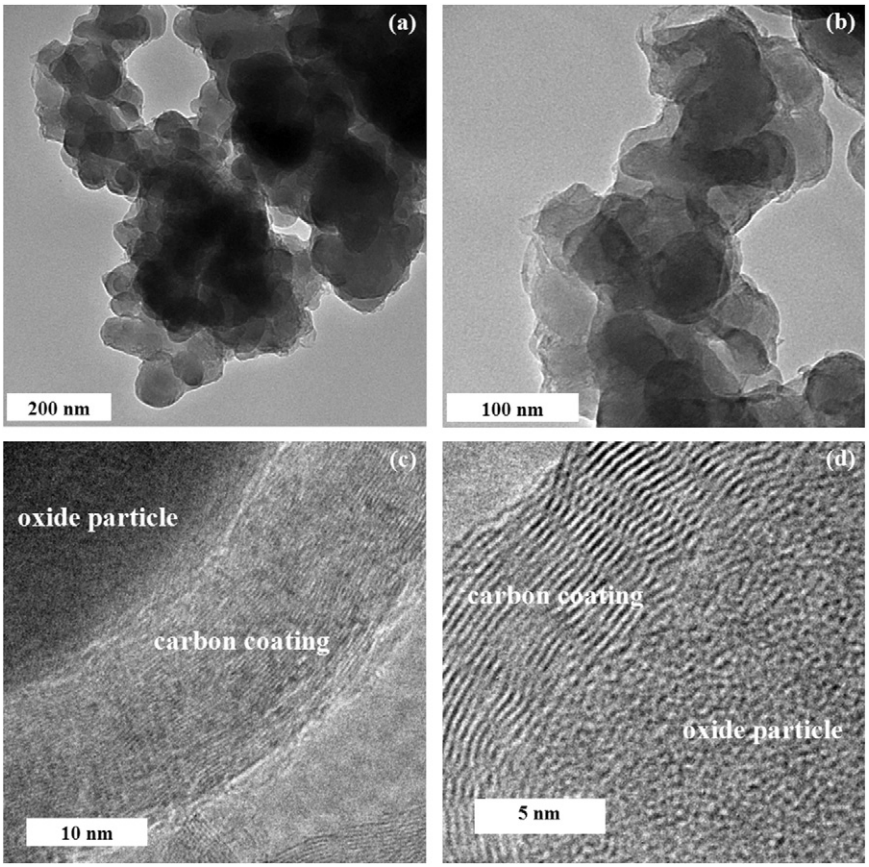

Fig. 6. HR-TEM images at various magnifications of the product obtained from the oxide mixture after heating to 1300 K and holding at this temperature for 10 min in a flowing CH_4 atmosphere.

4.2.2. Carbothermal reduction

Fig. 7 displays the XRD patterns of the products obtained at 1800 K for 60 min from the C coated oxide powders with various C contents. When the starting powder with 17.81 wt% C was used, a major TiC phase containing oxygen and traces of Ti_2O_3 and SiO_2 phases are seen. A higher C content of 24.93 wt% leads to disappearance of Ti_2O_3 peaks and a decrease in the intensity of SiO_2 peak at 22°. Also, TiC peak positions moved to the lower diffraction angles owing to enhanced carbothermal reduction as expected. When the C content was increased to 30.05 wt%, the diffraction peaks from the (002), (101), (104), (008), (105), (109) and (1012) crystal planes of hexagonal Ti_3SiC_2 phase appears at 10.0°, 34.1°, 39.5°, 40.8°, 42.5°, 58.4° and 73.5°, respectively. In this product, Ti_3SiC_2 phase co-exists with a major TiC phase and a minor SiC phase as seen from the pattern. In the case of using a higher C content (34.08 wt%) reactant, the peak intensities of the ternary carbide phase decrease, while those of TiC increase. In addition, SiC peaks become distinguishable in the pattern.

The results indicate that the use of the C coated oxide with 30.05 wt% C is more efficient for enhanced ternary carbide formation compared to the others. Hence, 30.05 wt% C, which is slightly above the thermodynamically predicted value (26.86 wt%), appears to be a good selection to study the effect of time on the formation of Ti_3SiC_2 phase at 1800 K.

Fig. 8 displays XRD patterns of the products obtained from the C coated oxide mixture with 30.05 wt% C for isothermal reaction periods ranging from 0 to 360 min. As can be seen from the patterns, TiC is a major phase in all products. At 0 min, SiO_2, Ti_3SiC_2 and SiC minor phases with faint diffraction peaks are seen. This indicates that significant carbothermal reduction takes place during heating to 1800 K. With increasing isothermal reaction time to 75 min, Ti_3SiC_2 peak intensities increase, while the SiO_2 peak disappears and SiC peaks remain faint. The ternary phase content of the product was estimated from the intensity ratio of the major peaks by an empirical formula developed by Zhang et.al. [9]. Integrated intensities (I) of (104) peak from Ti_3SiC_2 phase at 39.5° and (200) peak from TiC at 41.8° were used for the calculation, assuming that SiC content was negligible. The intensity ratio $I_{Ti_3SiC_2(104)}$:$I_{TiC(200)}$ was found to increase from ~0.01 at 0 min to 0.25 at 75 min. It was calculated that the product obtained at 75 min contains 31 wt% (32.8 vol%) Ti_3SiC_2. Beyond 75 min, the peak intensities from the ternary carbide phase gradually decrease and SiC peaks are clearly seen in the XRD pattern at 360 min. These results indicate that the ternary carbide decomposes into SiC and TiC for prolonged reaction times at 1800 K.

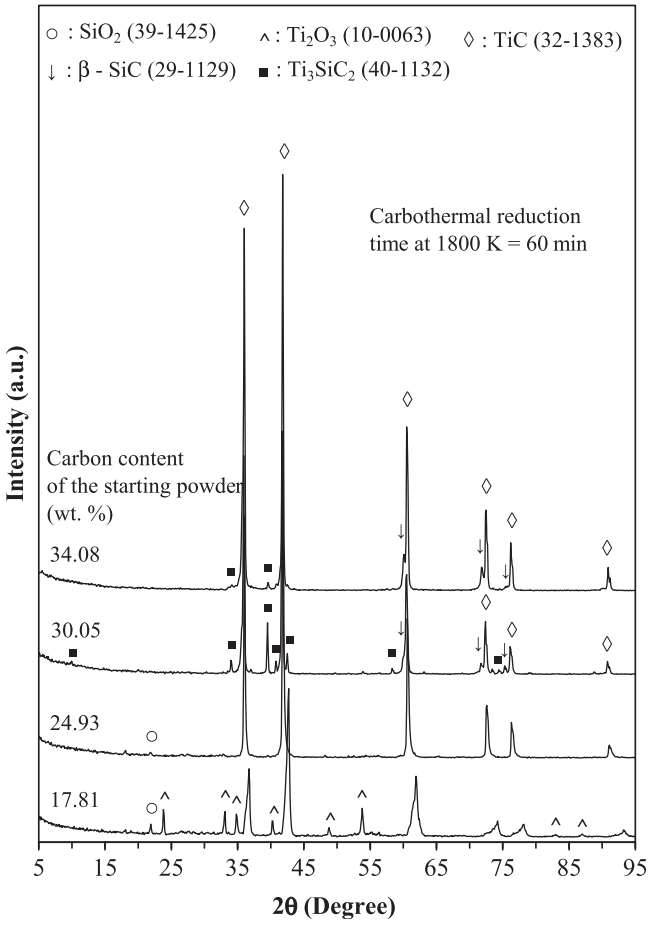

Fig. 7. XRD patterns of the products obtained from the C coated oxide mixtures with various C contents at 1800 K for 60 min.

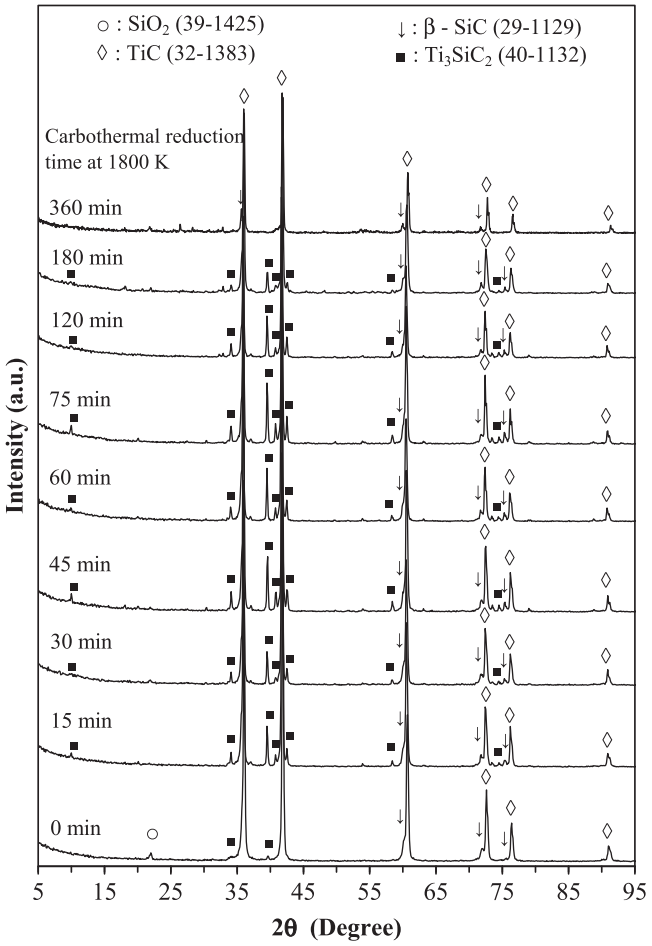

Fig. 8. XRD patterns of the products obtained from the C coated oxide mixture with C content of 30.05 wt% at 1800 K for various isothermal reaction times.

4.3. SEM and EDS analyses of the carbothermally reduced powders

Fig. 9 displays the morphologies of the carbothermally reduced products at 1800 K under various conditions. As seen from Fig. 9a, a flaky morphology is still present in the product obtained after heating the oxide mixture with graphite flakes to 1800 K. Fig. 9b–d displays the SEM images of the products synthesized from the oxide particles coated with C for isothermal reduction periods of 0, 75 and 360 min, respectively. At 0 min, the powder consists of nearly round particles with a mean size of 100 ± 46 nm (Fig. 9b). The image of the product at 75 min (Fig. 9c) reveals fine particles (111 ± 37 nm) and a few sintered particles of 1–2 μm. This sample also exhibits characteristic laminated crystals of the ternary carbide, as will be shown below by a higher magnification image and the corresponding EDS spectrum. At 360 min, highly sintered irregular shaped spongy chunks (> 10 μm) are present along with fine particles of 177 ± 52 nm (Fig. 9d).

Fig. 10a and b shows higher magnification SEM images of round particles and laminates present in the product with the largest amount of Ti_3SiC_2 phase along with the corresponding EDS spectra, respectively. Round particles exhibit intense Ti K_a (4.51 keV), C K_a (0.28 keV) and weak Si K_a (1.74 keV) X-ray peaks (Fig. 10a). This indicates that the particles essentially consist of titanium carbide phase. The thickness of laminated crystals is found to be in the range 30–60 nm. As can be seen from Fig. 10b, EDS spectrum of the laminates is comprised of the same elements, but Si K_a peak intensity is much higher. Hence, it is reasonable to ascribe nanolaminates to titanium silicon carbide ternary phase.

4.4. Reaction pathways to the formation of Ti_3SiC_2 compound

It was found that the use of C coated oxide powders resulted in the products with much higher Ti_3SiC_2 content compared to the oxide mixtures with graphite flakes. This is attributable to intimate contact between the reactants, which prompts the ternary carbide formation. Hence, it is plausible that carbothermal reactions start initially at the interface between carbon and the oxide particles, where there is a close contact between the solid reactants. Since the formation mechanism of the binary carbides is explained elsewhere [17,18], the present study will focus on the formation of Ti_3SiC_2 ternary compound.

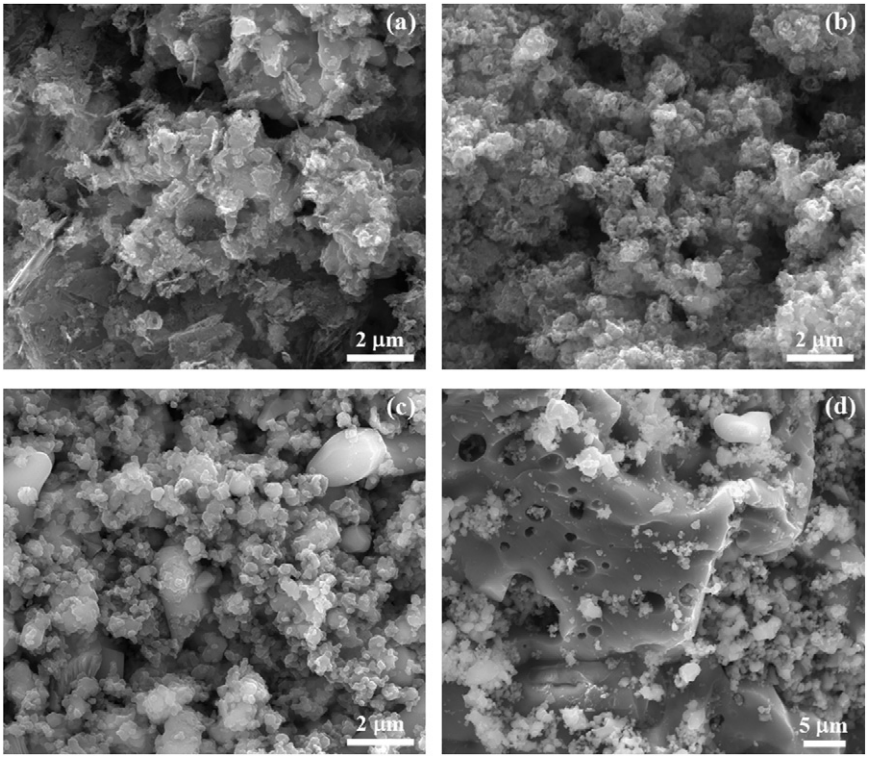

Fig. 9. SEM images of the carbothermally reduced products obtained at 1800 K from (a) the oxide mixture with graphite flakes (26.86 wt% C) and (b–d) the C coated oxide mixture (30.05 wt% C). Isothermal holding times were (a, b) 0 min, (c) 75 min and (d) 360 min.

In order to propose carbothermal reactions leading to the ternary carbide phase, changes in equilibrium compositions of condensed and gas phases with input carbon mole fraction (X_C) were analyzed in the TiO_2–SiO_2–C–Ar system. Fig. 11 shows the variation of gas phase composition in equilibrium with the condensed phases at 1800 K with X_C for a TiO_2:SiO_2 molar ratio of 1.5. The condensed phase fields represented by the numbers are separated by vertical dashed lines. As can be seen from Fig. 11, the main components of the gas phase are predicted to be Ar, CO and SiO in all condensed phase fields. CO has the highest amount among the gaseous products, and its concentration increases with X_C up to 0.75. The concentration of CO_2 is predicted to be much less than that of CO, while those of the other species (Si, TiO, SiO_2, TiO_2, O, Ti, SiC_2 and Si_2C) are found to be negligible.

As suggested by the thermodynamic calculations for X_C values up to 0.41, carbothermal reactions between the reactants will initially produce solid titanium sub-oxides (Ti_nO_{2n-1} phases with $n \geq 2$), gaseous SiO, CO and CO_2 species.

CO_2 may be formed in accordance with the following reactions:

$$SiO_{2(s)} + 1/2C_{(s)} \rightarrow SiO_{(g)} + 1/2CO_{2(g)} \quad (1)$$

$$nTiO_{2(s)} + 1/2C_{(s)} \rightarrow Ti_nO_{2n-1(s)} + 1/2CO_{2(g)} \quad (2)$$

CO_2 product will be consumed by free C through the Boudouard reaction producing CO:

$$SiO_{2(s)} + C_{(s)} \rightarrow SiO_{(g)} + CO_{(g)} \quad (3)$$

Since CO content is the highest among the gaseous products, possible reactions for the formation of SiO and Ti_nO_{2n-1} ($n \geq 2$) are given by the following net equations obtained from the sums of reaction (1) or (2) and (3):

$$SiO_{2(s)} + C_{(s)} \rightarrow SiO_{(g)} + CO_{(g)} \quad (4)$$

$$nTiO_{2(s)} + C_{(s)} \rightarrow Ti_nO_{2n-1(s)} + CO_{(g)} \quad (5)$$

As input C mole fraction increases from 0.41 to 0.69, Ti_3SiC_2 phase forms as a result of enhanced carbothermal reduction. The ternary carbide may form via reactions of solid titanium sub-oxide (Ti_2O_3) and C with gaseous SiO specie. The reactions are given by Eqs. (6) and (7).

$$3Ti_2O_{3(s)} + 2SiO_{(g)} + 19/2C_{(s)} \rightarrow 2Ti_3SiC_{2(s)} + 11/2CO_{2(g)} \quad (6)$$

$$3Ti_2O_{3(s)} + 2SiO_{(g)} + 15C_{(s)} \rightarrow 2Ti_3SiC_{2(s)} + 11CO_{(g)} \quad (7)$$

It is believed that the direct formation of Ti_3SiC_2 by the reactions (6) and (7) is sluggish because the reactions are limited to the solid contact points between C and Ti_2O_3. Hence, Ti_3SiC_2 formation is more probable when gaseous SiO and CO species react with Ti_2O_3 owing to increased contact area between these species. In this case, ternary carbide formation may take place via Eq. (8).

$$3Ti_2O_{3(s)} + 2SiO_{(g)} + 19CO_{(g)} \rightarrow 2Ti_3SiC_{2(s)} + 15CO_{2(g)} \quad (8)$$

CO_2 produced by reaction (6) or (8) is then reduced to CO via reaction (3). It should be noted that sum of these reactions yields reaction (7).

Based on these results, it is plausible to propose that Ti_3SiC_2 form from the oxide and carbon reactants in accordance with the overall reaction (9), which is the sum of Eqs. (4), (5) and (7).

$$3TiO_{2(s)} + 2SiO_{2(s)} + 11C_{(s)} \rightarrow Ti_3SiC_{2(s)} + SiO_{(g)} + 9CO_{(g)} \quad (9)$$

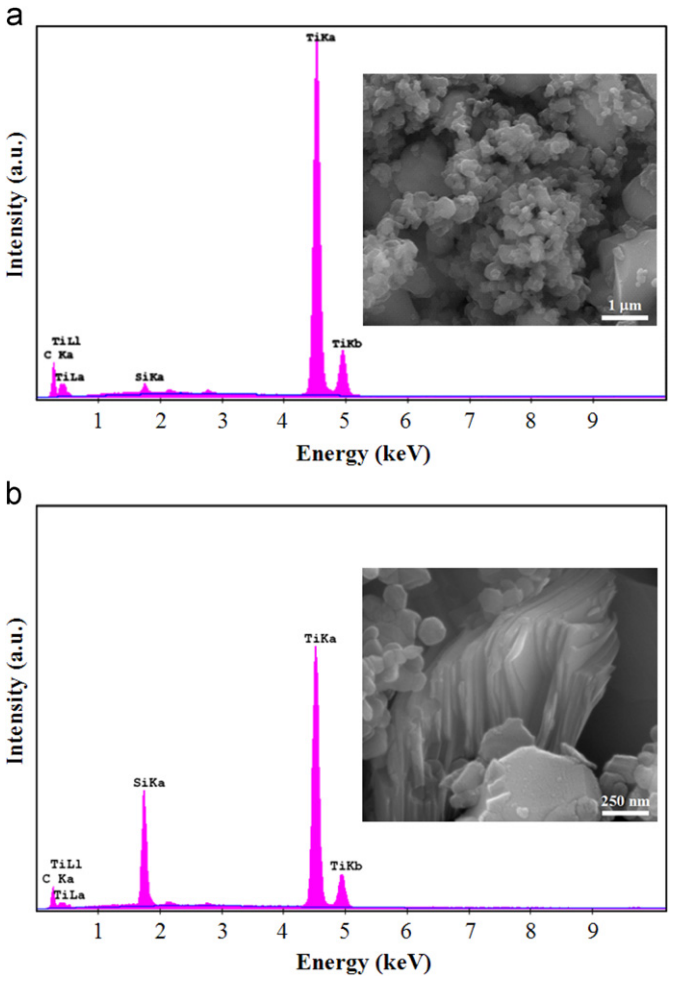

Fig. 10. SEM images at high magnifications and the corresponding EDS spectra of the product synthesized by carbothermal reduction of C coated oxide mixture with 30.05 wt% C at 1800 K for 75 min.

5. Conclusions

Equilibrium thermodynamic analysis revealed that Ti_3SiC_2 could be synthesized by carbothermal reduction technique from TiO_2, SiO_2 and C reactants with TiO_2:SiO_2 molar ratios ranging from 0.25 to 1.90 at 1800 K in Ar atmosphere. As the TiO_2:SiO_2 molar ratio increases in this range, the C content of the input reactant required for the formation of single Ti_3SiC_2 phase is predicted to raise from 58.33 to 69.80 mol%. C content of 68.75 mol% (26.86 wt%) was determined for the reactant with a TiO_2:SiO_2 molar ratio of 1.5 based on the thermodynamic prediction. The reactant with this composition yielded a trace amount of Ti_3SiC_2 along with major TiC and minor SiC phases at 1800 K, when graphite was used as a carbon source. Pyrolytic carbon shells (5–20 nm in thickness) grown on mixed oxide (molar ratio 1.5) particles by chemical vapor deposition from CH_4 was used as an alternative C supply in order to enhance Ti_3SiC_2 formation. Optimum C content for the C coated oxide mixtures was found to be 30.05 wt% at 1800 K for 60 min. The amount of Ti_3SiC_2 phase in the product obtained from this composition was observed to increase with time to 31 wt% at 75 min beyond which it gradually decreased. The powder with the highest ternary carbide content essentially consisted of spherical fine TiC particles and Ti_3SiC_2 nanolaminates.

Equilibrium thermodynamic analysis was used to propose the thermochemical reactions leading to Ti_3SiC_2 in the TiO_2–SiO_2–C–Ar system. It was anticipated that reaction of Ti_2O_3 with SiO and CO gases may play a dominant role in the formation of Ti_3SiC_2. This study demonstrates that Ti_3SiC_2 phase can be synthesized from TiO_2 and SiO_2 mixture by carbothermal reduction method, provided that there is intimate contact between the oxide reactants and C. Furthermore, the process described here has inherent advantages including a simple flexible synthesis procedure and low cost reactants, providing a sound rationale for massive production of Ti_3SiC_2 powder.

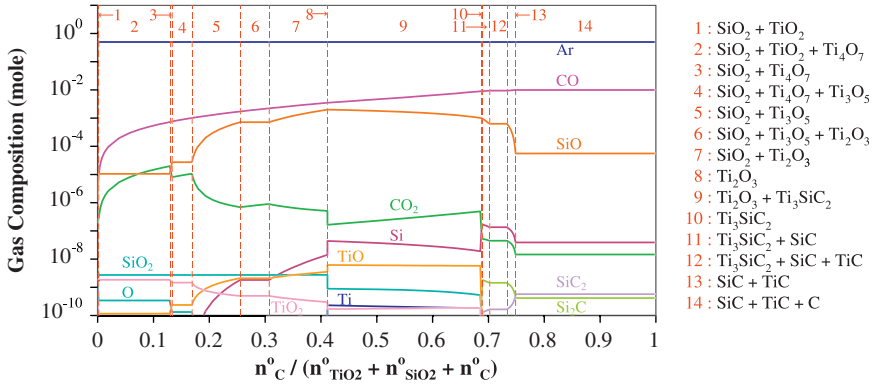

Fig. 11. Variation of equilibrium gas composition with input C mole fraction in the TiO_2–SiO_2–C system with a TiO_2:SiO_2 molar ratio of 1.5 at 1800 K for 0.5 mol Ar. Input TiO_2:Ar molar ratio is 0.006. Vertical dashed lines separate the condensed phase fields represented by the numbers.

References

[1] M.W. Barsoum, The $M_{N+1}AX_N$ phases: a new class of solids; thermodynamically stable nanolaminates, Progress in Solid State Chemistry 28 (2000) 201–281.

[2] M.W. Barsoum, T. El-Raghy, The MAX phases: unique new carbide and nitride materials, American Scientist 89 (2001) 334–343.

[3] P. Eklund, M. Beckers, U. Jansson, H. Högberg, L. Hultman, The $M_{n+1}AX_n$ phases: materials science and thin-film processing, Thin Solid Films. 518 (2010) 1851–1878.

[4] Z.M. Sun, Progress in research and development on MAX phases: a family of layered ternary compounds, International Materials Reviews 56 (2011) 143–166.

[5] S. Arunajatesan, A.H. Carim, Synthesis of titanium silicon carbide, Journal of the American Ceramic Society 78 (1995) 667–672.

[6] H. Fakih, S. Jacques, O. Dezellus, M.P. Berthet, F. Bosselet, M. Sacerdote-Peronnet, J.C. Viala, Phase equilibria and reactive chemical vapor deposition (RCVD) of Ti_3SiC_2, Journal of Phase Equilibria and Diffusion 29 (2008) 239–246.

[7] N.F. Gao, Y. Miyamoto, D. Zhang, Dense Ti_3SiC_2 prepared by reactive HIP, Journal of Materials Science 34 (1999) 4385–4392.

[8] J. Zhang, L. Wang, L. Shi, W. Jianga, L. Chena, Rapid fabrication of Ti_3SiC_2-SiC nanocomposite using the spark plasma sintering-reactive synthesis (SPS-RS) method, Scripta Materialia 56 (2007) 241–244.

[9] Z.F. Zhang, Z.M. Sun, H. Hashimoto, Rapid synthesis of ternary carbide Ti_3SiC_2 through pulse-discharge sintering technique from Ti/Si/TiC powders, Metallurgical and Materials Transactions A: Physical Metallurgy and Materials Science 33 (2002) 3321–3328.

[10] M. Zakeri, M.R. Rahimipour, A. Khanmohammadian, Effect of the starting materials on the reaction synthesis of Ti_3SiC_2, Ceramics International 35 (2009) 1553–1557.

[11] V. Pasumarthi, Y. Chen, S.R. Bakshi, A. Agarwal, Reaction synthesis of Ti_3SiC_2 phase in plasma sprayed coating, Journal of Alloys and Compounds 484 (2009) 113–117.

[12] V. Gauthier, B. Cochepin, S. Dubois, D. Vrel, Self-propagating high-temperature synthesis of Ti_3SiC_2: study of the reaction mechanisms by time-resolved X-ray diffraction and infrared thermography, Journal of the American Ceramic Society 89 (2006) 2899–2907.

[13] G. Eriksson, Thermodynamic studies of high temperature equilibrium, Chemica Scripta 8 (1975) 100–103.

[14] T.M. Besmann SOLGASMIX-PV, A Computer Program to Calculate Equilibrium Relationships in Complex Chemical Systems, Report No: ORNL/TM-5775, Oak Ridge National Laboratory, 1977.

[15] M.W. Chase, C.A. Davies, J.R. Downey, D.J. Frurip, R.A. McDonald, A.N. Syverud, JANAF Thermochemical Tables, third ed., Journal of Physical and Chemical Reference Data 14 (Suppl. l), 1985.

[16] O. Knacke, O. Kubaschewski, K. Hesselmann, Thermochemical Properties of Inorganic Substances, second ed., Springer-Verlag, Berlin Heildelberg, 1991.

[17] S. Cetinkaya, S. Eroglu, Chemical vapor deposition of carbon on particulate TiO_2 from CH_4 and subsequent carbothermal reduction for the synthesis of nanocrystalline TiC powders, Journal of the European Ceramic Society 31 (2011) 869–876.

[18] S. Cetinkaya, S. Eroglu, Chemical vapor deposition of C on SiO_2 and subsequent carbothermal reduction for the synthesis of nanocrystalline SiC particles/whiskers, International Journal of Refractory Metals and Hard Materials 29 (2011) 566–572.